Thermal Impedance Spectroscopy Method as Applied for Road Bearing Layer Structure Thermoelectric Parameters Determination

Youssou Traore[#1,2], Alassane Ba[*2],CheikhThiam[*2], M. S. Ould Brahim[#1],Moussa Dieng[#1] , Ould Mohamed Bah[#1], Issa Diagne[#1], Gregoire Sissoko[#1]

[#1]*Laboratoire des Semi-conducteurs et d'Energie Solaire, Faculté des Sciences et Techniques, Université Cheikh AntaDiop, Dakar, Sénégal*

[#2]*Ecole Polytechnique de Thiès, Sénégal*

Abstract:

In this article, we propose to determine by thermal electric- analogy of the thermoelectric parameters of a road bearing layer structure from the thermal impedance spectroscopy method.

When the road surface is submitted to thermal constraints, a heat exchange phenomenon appears to be characterized by the radiation thermal exchange coefficient and the convection thermal exchange coefficient. The influenceof one of these coefficients compared with the other one on the road depends on its environment (shade or illumination).

The determination of the thermal electric parameters allow the valid bearing layer thermal stability. The method used is the thermal impedance spectroscopy method.

Keywords:*Road- thermal impedance spectroscopy- convection thermal exchange coefficient- radiation thermal exchange coefficient.*

I. INTRODUCTION

The road structure can be considered as a set of multilayer. A road surface get permanently thermal [1-3] and mechanical constraints [4,5]. Many scientifichas been done in the aim of studying the impact of heavy weighted (car) on the road surface dimensioning, from the deformation module and the permissible stresses [6-8].

The noted damages on the road [9,10] appears in the form of cracks or of excessive deformations [11,12].

In zones of high temperature, it is primordial to take in account this phenomenon for the road conception, maintenance and rehabilitation. So, other others has lead there studies in the effect of the temperature on the road's body [13-16]. The amplitude of this phenomenon depends on several parameters, but specially the soil characteristics (granulate, permeability, chemical physical composition, amount of water, density, level of saturation…)[17] and external factors (weather conditions and water supply) [10].

Scientifique research deals with this problem through modeling and analogic studies. However, the thermal impedance spectroscopy [18-20] seemstoo relevant to the thermal stability of systems.

The aim of this paper is to propose the thermal electric parameters such as the break frequency, the resonance frequency, the series and parallel resistance by thermal electric analogy. This study highlights the convection thermal exchange coefficient[21-22] in shadowed zones, and radiation thermal exchange coefficient [23, 24] in zones under illumination.

II. MODEL STUDY

The studied model is a road structure. Its body consists of a multilayer system composed by an asphalt coat [25] on the surface layer, a crushed gravel material as the based layer, and a raw lateritic foundation. These materials are supported by the based soil as indicated in figure 1.

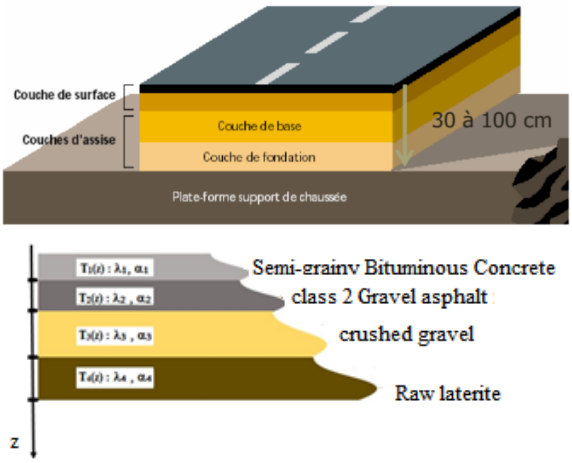

Figure 1: View of the Road Structure

The thickness of the layers is the following:

- Bituminous Semi-Grenu Concrete : 0.05m
- Class 2 Gravel Asphalt: 0.08m
- Crushed Gravel : 0.2m
- Raw Laterite : 0.2m

When the most external layer of the road subjected (submitted) is submitted to thermal constraint (figure 2), we observe then a heat transfer phenomenon from high towards low temperatures.

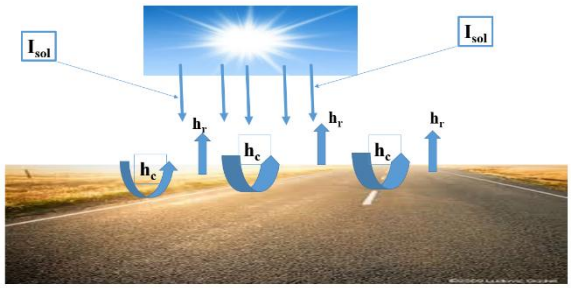

Figure 2:Constraints and Thermal Exchanges on the Asphalt

The indications i=1,2,3,4 are respectively attributed from the first to the last layer. To determine the coefficients $A_i(h1,h2,\omega,t,Cn)$and $B_i(h1,h2,\omega,t,Cn)$, we are going to define the conditions on the borders.

This phenomenon creates thermal exchanges governed by the equation of the heat (1)

$$\frac{\partial^2 T(z,hc,hr,\omega,t,Cn)}{\partial z^2} - \frac{1}{\alpha}\frac{\partial T(z,hc,hr,\omega,t,Cn)}{\partial t} = Pp(1)$$

The heat equations relative to every layer are proposed by considering that there is no internal source of heat:

In the of Semi-grainy Bituminous concrete layer

$$\frac{\partial^2 T_1(z,hc,hr,\omega,t,Cn)}{\partial z^2} - \frac{1}{\alpha_1}\frac{\partial T_1(z,hc,hr,\omega,t,Cn)}{\partial t} = 0(2)$$

In the connection layer of class 2 Gravel Asphalt of

$$\frac{\partial^2 T_2(z,hc,hr,\omega,t,Cn)}{\partial z^2} - \frac{1}{\alpha_2}\frac{\partial T_2(z,hc,hr,\omega,t,Cn)}{\partial t} = 0(3)$$

In the basic layer crushed gravel

$$\frac{\partial^2 T_3(z,h1,h2,\omega,t,Cn)}{\partial z^2} - \frac{1}{\alpha_3}\frac{\partial T_3(z,h1,h2,\omega,t,Cn)}{\partial t} = 0(4)$$

In the layer of foundation in Raw Laterite

$$\frac{\partial^2 T_4(z,h1,h2,\omega,t,Cn)}{\partial z^2} - \frac{1}{\alpha_4}\frac{\partial T_4(z,h1,h2,\omega,t,Cn)}{\partial t} = 0(5)$$

With $\alpha_1 = \frac{\lambda_1}{\rho_1 c_1}$; $\alpha_2 = \frac{\lambda_2}{\rho_2 c_2}$; $\alpha_3 = \frac{\lambda_3}{\rho_3 c_3}$ and $\alpha_4 = \frac{\lambda_4}{\rho_4 c_4}$

- ✓ $T_1(z,hc,hr,\omega,t,Cn)$: temperature in a considered point in the Grainy Semi Bituminous Concrete
- ✓ $T_2(z,hc,hr,\omega,t,Cn)$: temperature in a considered point in class 2 Gravel Asphalt
- ✓ $T_3(z,hc,hr,\omega,t,Cn)$: temperature in a considered point in the Crushed Gravel
- ✓ $T_4(z,hc,hr,\omega,t,Cn)$: the temperature in a point considered in the Raw Laterite

However, we meet three types of boundary conditions:

- ➢ The boundary conditions told condition imposed flow (problem of Neumann)
- ➢ The boundary conditions told condition imposed flow (problem of Neumann)
- ➢ The boundary conditions said condition of Fourier or Newton (problem of Fourier)

The heat transfers in this domain are conductive and monodimensional.

In the interface outer environment and the layer of bituminous concrete, a condition of continuity of flows is held:

- ❖ Interface outer environment and the layer of Grainy Semi Bituminous Concrete:

$$-\lambda_1 \frac{\partial T_1(z)}{\partial z}\Big|_{z=0} = hc\big(Ta1 - T(0)\big) + hr\big(T_s - T0 + Isol(6)$$

- ✓ hc:Coefficient of thermal exchange by convection
- ✓ hr :coefficient of thermal exchange by radiation
- ✓ Ta1 : ambient temperature of the environment
- ✓ Ts : temperature supplied by the sun in the ambient environment.
- ✓ Isol : solar flow arriving on the surface of the first layer

The expression of the solar flow is proposed by the following [11,12] :

$$I_{sol} = (0.828.\mathrm{I} + \mathrm{b}).(1 - \mathrm{Cn}/100)(7)$$

So the cloud layer allows estimate the quantity of light which reaches the surface of the ground.

- ❖ Grave Asphalt of class 2 Interface between the Grainy Semi Bituminous Concrete and crushed gravel:

$$\lambda 1 \frac{\partial T1(z)}{\partial z}\Big|_{z=L1} = \lambda 2 \frac{\partial T2(z)}{\partial z}\Big|_{z=L1}(8)$$

$$T1(L1) = T2(L1)(9)$$

- ❖ Interface between class 2 Gravel Asphalt and the Crushed Gravel:

$$-\lambda_2 \frac{\partial T2(z)}{\partial z}\Big|_{z=L2} = -\lambda_3 \frac{\partial T3(z)}{\partial z}\Big|_{z=L2}(10$$

$$T2(L2) = T3(L2)(11)$$

- ❖ Interface between the Crushed Gravel and the Raw Laterite: :

$$-\lambda_3 \frac{\partial T3(z)}{\partial z}\Big|_{z=L3} = -\lambda_4 \frac{\partial T4(z)}{\partial z}\Big|_{z=L3}(12)$$

$$T3(L3) = T4(L3) \qquad (13)$$

- ❖ Interface between the Raw Laterite and the platform: :

$$-\lambda_4 \frac{\partial T4(z)}{\partial z}\Big|_{z=L4} = 0(14)$$

$$T4(L4) = Tp(15)$$

At the initial moment, the temperature in a layer is isothermal. But this initial temperature is not

constant for the set of layers. Indeed we supposed a one degree variation between layers: of the bearing layer to the layer of platform. So, by taking into account this temperature, we proceed to a change of variables .

In the layer of Semi-grainy Bituminous concrete rotation

$$\bar{T}_1(z,h1,h2,\omega,t,Cn) = T_1(z,h1,h2,\omega,t,Cn) - T_{i1}$$

In the connection layer of class 2 Gravel Asphalt

$$\bar{T}_2(z,h1,h2,\omega,t,Cn) = T_2(z,h1,h2,\omega,t,Cn) - T_{i2}$$

In the basic layer of crushed gravel

$$\bar{T}_3(z,h1,h2,\omega,t,Cn) = T_3(z,h1,h2,\omega,t,Cn) - T_{i3}$$

In the foundation layer of Raw Laterite

$$\bar{T}_4(z,h1,h2,\omega,t,Cn) = T_4(z,h1,h2,\omega,t,Cn) - T_{i4} \quad (19)$$

The heat equation becomes:

In the layer of Semi-grainy Bituminous concrete

$$\frac{\partial^2 \bar{T}_1(z,h1,h2,\omega,t,Cn)}{\partial z^2} - \frac{1}{\alpha_1}\frac{\partial \bar{T}_1(z,h1,h2,\omega,t,Cn)}{\partial t} = 0 \quad (20)$$

In the class 2 connection layer of Gravel Asphalt

$$\frac{\partial^2 \bar{T}_2(z,h1,h2,\omega,t,Cn)}{\partial z^2} - \frac{1}{\alpha_2}\frac{\partial \bar{T}_2(z,h1,h2,\omega,t,Cn)}{\partial t} = 0 \quad (21)$$

In the basic layer crushed gravel

$$\frac{\partial^2 \bar{T}_3(z,h1,h2,\omega,t,Cn)}{\partial z^2} - \frac{1}{\alpha_3}\frac{\partial \bar{T}_3(z,h1,h2,\omega,t,Cn)}{\partial t} = 0 \quad (22)$$

In the foundation layer in Raw Laterite

$$\frac{\partial^2 \bar{T}_4(z,h1,h2,\omega,t,Cn)}{\partial z^2} - \frac{1}{\alpha_4}\frac{\partial \bar{T}_4(z,h1,h2,\omega,t,Cn)}{\partial t} = 0 \quad (23)$$

The resolution of these equations from the method of separation of variables gives the expression of the additional temperature under the following shape:

$$\bar{T}_i(z,hc,hr,\omega,t,Cn) = (A_i(hc,hr,\omega,t,Cn)\sinh(\beta_1.z) + B_i(hc,hr,\omega,t,Cn)\cosh(\beta_1.z)) * e^{j.\omega.t} \quad (24)$$

➢ **Heat density flow and thermal impedance.**

The quantity of per unit square is obtained from the Fourier law by conduction [28-30]:

$$\vec{\phi}_i(z,h1,h2,\omega,t,Cn) = -\lambda_i.\overrightarrow{grad}T_i(z,h1,h2,\omega,t,Cn) \quad (25)$$

In frequency modulation, the dynamic impedance [31] is given in electricity by the following expression:

$$Z_n(\lambda,\omega,Sf_n,Sb_n) = \frac{V_n(\lambda,\omega,Sf_n,Sb_n)}{J_n(\lambda,\omega,Sf_n,Sb_n)} \quad (26)$$

By analogy, the equivalent [32,33] thermal impedance expression is deducted from two distinct points given by.:

$$Z_{eq}(x,h1,h2,\omega,t) = \frac{\Delta T(x,h1,h2,\omega,t)}{\Phi(x,h1,h2,\omega,t)} \quad (27)$$

We shall note the correspondence existencebetween thermal electric parameters. The following table illustratesthese relations:

Table 1 : Correspondence Between Thermal Electric Parameters

ELECTRIC PARAMETERS	THERMIC PARAMETERS
Potentiel difference (Volt) : ΔV	Temperature difference (°C) : ΔT
Curent density (A.m^{-2}) : $J = \frac{dq}{dt}$	Heat flow density (W.m^{-2}) : $\bar{\Phi} = -\lambda\overrightarrow{grad}T$ (18)
Electrique impedance (W) : $Z = \frac{\Delta V}{J}$	Thermal impedance (K/W.m^{-2}) : $Z_{eq} = \frac{\Delta T}{\Phi}$
Currentintensity (A) : I	Heat flow (W) : φ

III. RESULTS AND DISCUSSIONS

A. *Bode Diagram of the Thermal Equivalence Impedance*

The figures 3 and 4, give the thermal equivalence module under influence the radiation thermal exchange coefficient and the convection thermal exchange. These curves give the break frequency, the resonance frequency, and highlight the frequency band regime.

Indeed, for long solicitation periods (weak pulse values), the equivalence thermal impedance is so low that seems to be constant as a statistic regime. A pert from some values called break frequency, it is noticed a rise of the thermal impedance reaching a maximum and decrease. This part in the curve, correspond to dynamic regime.

Tables 2and3 give the break frequency values, the resonance, the equivalentthermal impedance module maximum amplitude.

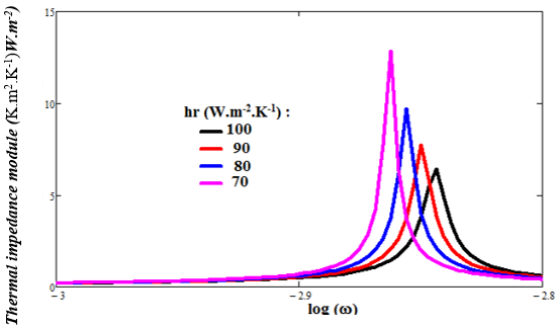

Figure 3:Equivalent Thermal Impedance Module According to the Decimal Logarithm of the Pulse. Hc=0.01W.M^{-2}.K^{-1}, I=800W.M^{-2}, Z=0.05m

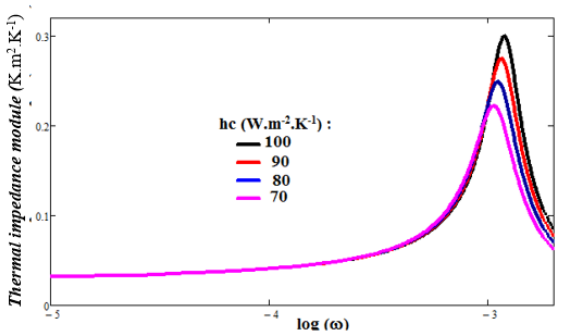

Figure 4:Equivalent Thermal Impedance Module According to the Decimal Logarithm of the Pulse Hr=0.01W.M^{-2}.K^{-1}, I=800W.M^{-2}, Z=0.05m

Table2: Break Frequency Values and Resonance Under Influence of the Radiation Thermal Exchange Coefficient

	radiation thermal exchange coefficient (W.m^{-2}.K^{-1})			
	100	90	80	70
Break frequency (rad/s)	$10^{-2.881}$	$10^{-2.874}$	$10^{-2.868}$	$10^{-2.862}$
	$10^{-2.840}$	$10^{-2.837}$	$10^{-2.831}$	$10^{-2.826}$
Resonance frequency (rad/s)	$10^{-2.862}$	$10^{-2.855}$	$10^{-2.849}$	$10^{-2.843}$
Ze_{max}(K.m^2.W^{-1})	10.833	9.689	7.711	6.400

Table3:Break Frequency Values and Resonance For Different Value of Convection Thermal Exchange Coefficient

	convection thermal exchange coefficient (W.m-2.K-1)			
	100	90	80	70
Break frequency (rad/s)	$10^{-3.371}$	$10^{-3.371}$	$10^{-3.371}$	$10^{-3.371}$
Resonance frequency (rad/s)	$10^{-2.926}$	$10^{-2.936}$	$10^{-2.954}$	$10^{-2.971}$
Ze_{max}(K.m^2.W^{-1})	0.299	0.274	0.249	0.222

B. Bode Diagramm of the Equivalent Impedance Phase

Figures5and6allow give conclusion on the thermal behavior of bearing layer. We notice a frequency band in whichn, the thermal impedance phase is positive showing the predominance of inductive effect. For these frequency the amount of heat received by the bearing layer is dissipated through the other layers.

For the negative values ofrequency in which the phase is negative, (predominance of capacitive effets), the bearind layer restore the heat flow.The values equal to zero are related on the resonance.

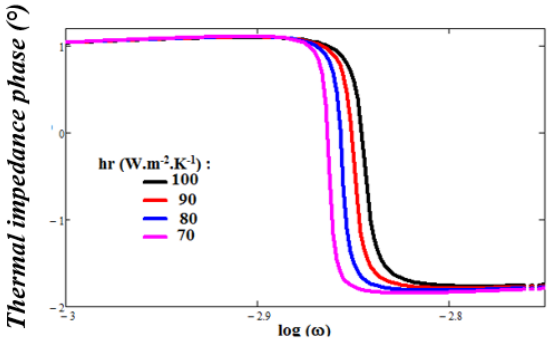

Figure 5: Equivalent Thermal Impedance Phase According to the Decimal Logarithm of the Pulse. Hc=0.01W.M^{-2}.K^{-1}, I=800W.M^{-2}, Z=0.05m

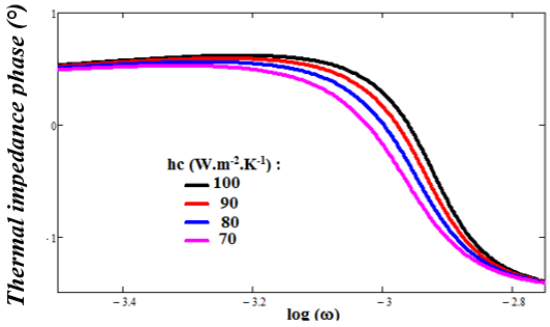

Figure 6: Equivalent Thermal Impedance Phase According to the Decimal Logarithm of the Pulse. Hc=0.01W.M^{-2}.K^{-1}, I=800W.M^{-2}, Z=0.05m

C. Nyquist Representation of the Equivalent Thermal Impedance

The NYQUIST representation confirms results got from Bode diagramand the phase [34]. It permits to validate the stability of a system.

In illumination zone, thermal impedance curves present both the capacitive and inductive predominance. These two phenomena are separated by the resonance. For this weather condition, the bearing layer reaches its thermal stability.

The frequency limit values allow having the thermoelectric parameter in the corresponding layer. Indeed, the shunt resistance corresponds to the double of the imaginary part maximum of the thermal impedance. For the parallel resistance, it corresponds to the real part when the imaginary part is equal to zero.

In shadowed zone, the series resistance is added to the preceding parameters, translating heat losses in the layer by restitution.

Tables 4and 5 give the résistance values in the two zone.

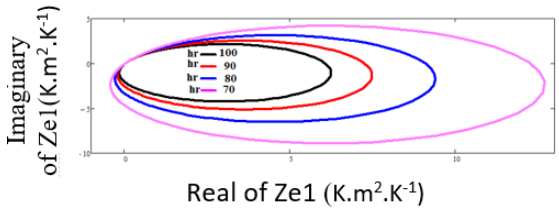

Figure 7: Thermal Impedance Imaginary Part According to the Real Part Under Influence of the Radiation Thermal Exchange Coefficient. Hc=0.01W.M^{-2}.K^{-1}, I=800W.M^{-2}, Z=0.05m

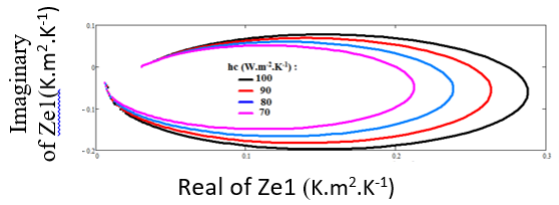

Figure 8: Thermal Impedance Imaginary Part According to the Real Part Under Influence of the Convection Thermal Exchange Coefficient. Hr=0.01W.M^{-2}.K^{-1}, I=800W.M^{-2}. Z=0.05m

Table 4: Parallel and Shunt Resistance Under Influence of Radiation Thermal Exchange Coefficient

	radiation thermal exchange coefficient (W.m-2.K-1)			
	100	90	80	70
Parallel resistance (K.m^2.K^{-1})	6.15	7.21	9.14	12.21
Shunt resistance (K.m^2.K^{-1})	4.26	5.06	6.28	8.38

Table5: Resistances Parallel, Shuntandseriefor Different Value of convection Thermal Exchange Coefficient

	Convection thermal exchange coefficient(W.m^{-2}.K^{-1})			
	100	90	80	70
Parallel resistance (K.m^2.K^{-1})	0.240	0.220	0.190	0.170
Shunt resistance (K.m^2.K^{-1})	0.154	0.136	0.118	0.102
Series resistance(K.m^2.K^{-1})	0.02	0.02	0.02	0.02

D. Equivalent Electric Model

The equivalent electric circuit of the model is proposed by the two conditions:

- Equivalent electric model of the road in illuminated zone
- Equivalent electric model of the road in shadowed zone

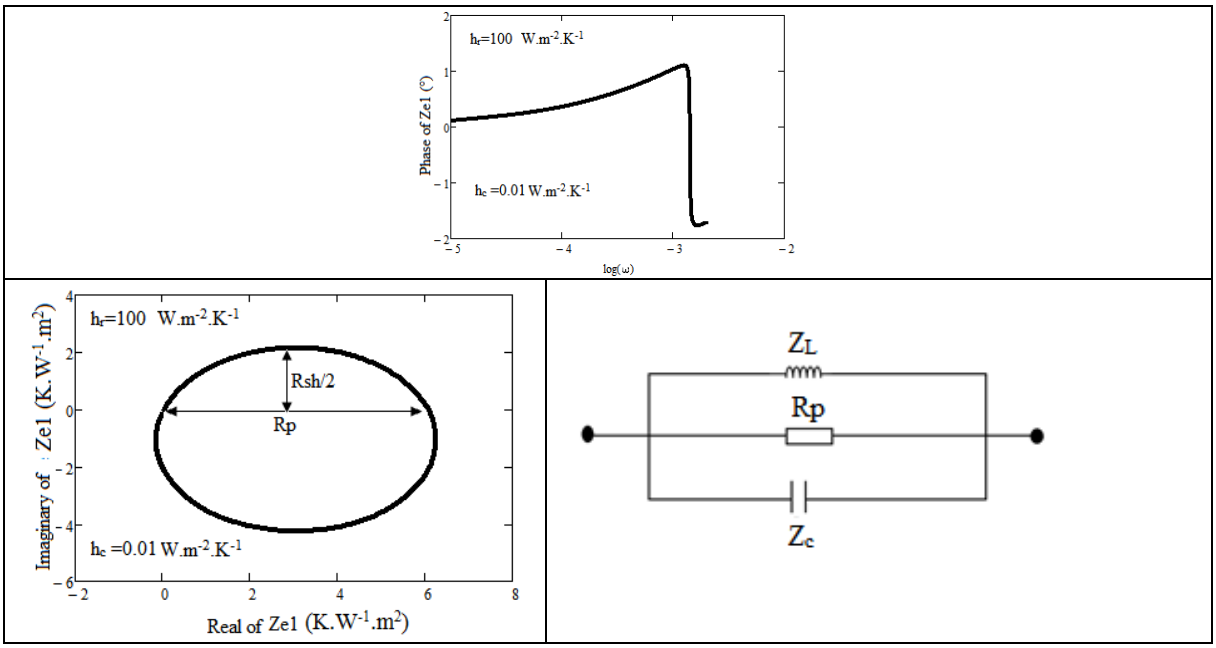

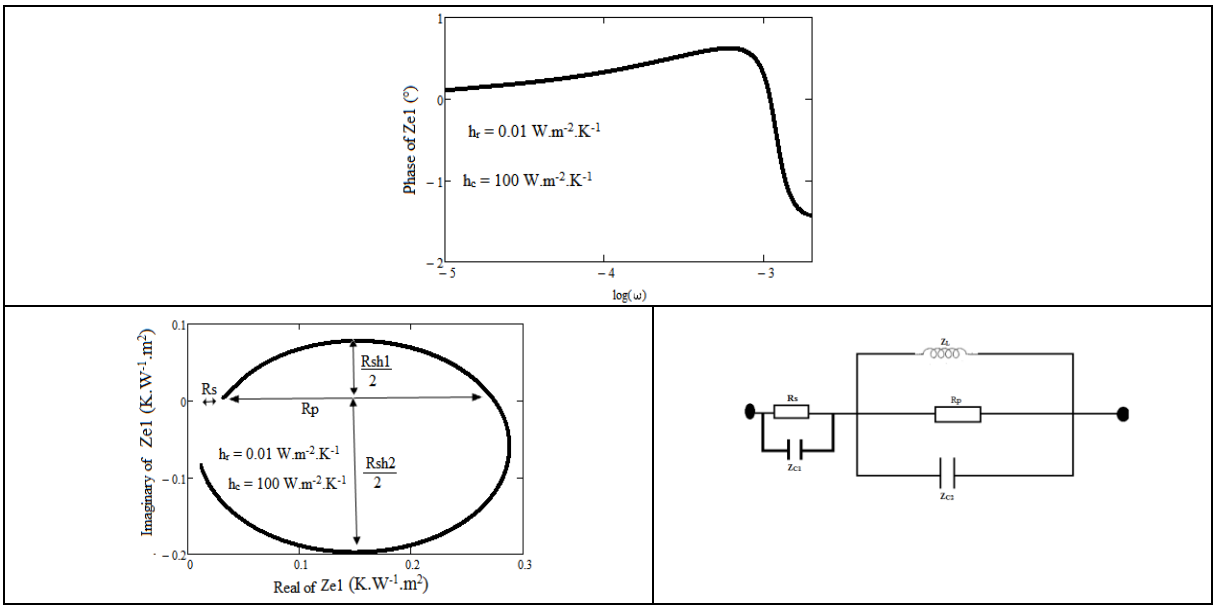

CONCLUSION

The thermal behavior modeling of the bearing road body has been done under illumination and shade. The thermal impedance spectroscopy study from Bode diagram, the phase and the NYQUIST representation has helped determining the break frequency, the resonance frequency ant series, shunt, parallel resistances.

The representation has allowed introducing equivalent electric models and giving conclusion relating on the bearing layer thermal stability.

REFERENCES

[1] A.Mammeri, L.Ulmet ,C.Petit , A.Mokhtari Modélisation d'un corps de chaussée rigide sous sollicitations thermiques en régime transitoire XXX e Rencontres Universitaires de Génie Civil. Chambéry, 6 au 8 juin 2012.

[2] Bissada, F., Asphalt pavement temperature related to Kuwait climate. Highway Research Record 404, Transportation Research Board, Washington, D.C., 1972, pp. 71-85.

[3] Al-Abdul, H.I., Balghunaim, F.A., Asphalt pavement temperature related to arid Saudi environment. Journal of Material in Civil Engineering, Volume 6, Issue 1, February 1994, pages 1-14.

[4] BECQUART F., « Caractérisation du comportement mécanique d'un mâchefer dans la perspective d'une méthologie de dimensionnement adaptée aux structures de chaussées. », XXIVème Rencontres Universitaires de Génie Civil –3ème Prix du Concours Jeunes Chercheurs, 2006.

[5] Adolphe KimbonguilaManounou, Frédéric Becquart, Nor-EdineAbriakMéthode de dimensionnement des structures de chaussées : quelle(s) adaptabilité(s) pour les matériaux granulaires alternatifs ?33èmes Rencontres de l'AUGC, ISABTP/UPPA, Anglet, 27 au 29 mai 2015

[6] FAKHARI TEHRANI F., ABSI J., ALLOU F., PETIT C., « Heterogeneous Numerical Modeling of Asphalt Concrete through Use of a Biphasic Approach: Porous Matrix/inclusions », Computational Materials Science, vol. 69, 2013, p. 186-196.

[7] MO L.T., HUURMAN M., WU S.P., MOLENAAR A., « Investigation into Stress States in Porous Asphalt Concrete on the Basis of FE-Modelling », Finite Elements in Analysis and Design, vol. 43, n° 4, 2007, p. 333-343.

[8] BONNOT, J., "La détermination des propriétés des matériaux en vue du dimensionnement des chaussées". Bulletin de liaison des laboratoires des ponts et chaussées, janvier-février 1973, n°63, pp.73-82.

[9] Rezqallah H. Ramadhan* Hamad I. Al-abdulwahhab., (1997)
Temperature variation of flexible and rigid pavement in Eastern audi Arabia. Building and environment, Vol.32,No. 4, pp. 367-373,

[10] Williamson, R. H., (1977) Effect of environment on pavement temperature. Proceedings of Third International Conference on Structural of Asphalt Pavements, Michigan, vol. 1, pp. 144-157

[11] I. Demir, H.M. Zbib, et M. Khaleel. (2001) Microscopic analysis of crack propagation for multiple cracks, inclusions and voids. Theoretical and Apllied fracture mechanics, 36:147–164.

[12] G.N King, H.W King, W. Arand O. Harders, et J.P. Planche. (1993) Influence of asphalt grade and polymer concentration on the low temperature performance of polymer modified asphalt. J.Assoc. Asphalt Paving Techn., 62:1–18.

[13] Solaimanian M, Kennedy TW. Prediction maximum pavement surface temperature using maximum air temperature and hourly solar radiation. Transport Res Rec: J Tranport Res Board 1993; 1417:1-11.

[14] Rezqallah H. Ramadhan* Hamad I. Al-abdulwahhab., Temperature variation of flexible and rigid pavement in Eastern Saudi Arabia. Building and environment, Vol. 32, No. 4, pp. 367-373, 1997.

[15] Williamson, R. H., Effect of environment on pavement temperature. Proceedings of Third International Conference on Structural of Asphalt Pavements, Michigan, 1977, volume 1, pp. 144-157.

[16] Youssou Traore, Séni Tamba, Alassane Diene, Khatry Ould Cheikh, Moussa Dieng, El hadjibalamoussanyakhaté, Issa DIAGNE, and Grégoire SISSOKO Etude du transfert de chaleur à travers une chaussée en régime dynamique fréquentiel : l'influence des paramètres extrinsèques International Journal of Innovation and AppliedStudies ISSN 2028-9324 Vol. 20 No. 2 May. 2017, pp. 616-623

[17] Moussa Wone, (1995) Contribution A La Modélisation Du Comportement Hydrique Et Mécanique Des Remblais Routiers En Matériaux Fins, thèse, l'Ecole Nationale des Ponts et Chaussées, spécialité : géotechnique,pp-148-150

[18] Defer D., Bellatar S, B. Duthoit, «Non destructive in situ inspection of a wall by thermal impedance » Materials and Structure, 26, 3-7, 1993

[19] I. Gaye, A. Corréa, A. L. Ndiaye, E. Nanéma, M. Adj, G. Sissoko."Impedance parameters determination of silicon solar cell using the one diode model in transient study". Renewable Energy, Vol 3, pp. 1598-1601, 1996.

[20] R. Anil Kumar, M.S. Suresh and J. Nagaraju. "Measurement of AC parameters of Gallium Arsenide (GaAs/Ge) solar cell by impedance spectroscopy", IEEE Transactions on Electron Devices, Vol.48, No.9, pp 2177-2179, September 2001.

[21] Xuan Y. and Roetzel W. 2000. Conceptions for heat transfer correlation of nanofluids. International Journal of Heat and Mass Transfer. 43: 3701-3707.

[22] Duangthongsuk W. and Wongwises S. 2010. An experimental study on the heat transfer performance and pressure drop of TiO2-water nanofluids flowing under a turbulent flow regime. International Journal of Heat and Mass Transfer. 53: 334-344.

[23] Hinojosa, J. F., Estrada, C. A., Cabanillas, R. E., and Alvarez, G. 2005. Numerical study of transient and steady-state natural convection and surface thermal radiation in a horizontal square open cavity, Numerical Heat Transfer A, vol. 48, 179-196.

[24] Hinojosa, J. F., Estrada, C. A., Cabanillas, R. E., and Alvarez, G. 2005. Nusselt number for the natural convection and surface thermal radiation in a square tilted open cavity, Int. Com. InHear and Mass Transfer, vol. 32, 1184-1192.

[25] Proteau M., Paquin Y., « Contribution de différents bitumes purs et bitumes modifiés par ajout de polymères à la résistance à l'orniérage », Routes et Aérodromes, N°793, 2001, p. 34-39.

[26] N. B. Guttman, J. D. Matthews, Computation of extraterrestrial solar radiation, solar elevation angle and true solar time of sunrise and sunset, SOLMET Vol. 2-Final report, National Climatic Center, U.S. Departement of Commerce (1979), 49-52.

[27] J. Schmetz, Relationship between solar net radiative fluxes at the top of the atmosphere and at the surface, Journal of the Atmospheric Sciences, 50-8 (1993), 1125.

[28] Turgut A., Tavman I., Chirtoc M., Schuchmann H. P., Sauter C. and Tavman S. 2009. Thermal conductivity and viscosity measurements of water-based TiO2 nanofluids. International Journal of Thermophysics. 30: 1213-1226.

[29] Buongiorno J., Venerus D. C., Prabhat N. and McKrell T. 2009. A benchmark study on the thermal conductivity of nanofluids. Journal of Applied Physics. 106: 094312.

[30] Murshed S. M. S., Leong K. C. and Yang C. 2005. Enhanced thermal conductivity of TiO2-water based nanofluids. International Journal of Thermal Sciences 44: 367-373.

[31] A.J. Steckl and S.P. Sheu (1979)
The a.c. admittance of the p-n PbS Si heterojunction
Solid-State Electronics Vol.23, pp. 715 – 720

[32] R. Anil Kumar, M.S. Suresh and J. Nagaraju
Measurement of AC parameters for Gallium Arsenide (GaAs/Ge) solar cell by impedance spectroscopy
IEEE Transactions on Electron Devices, Vol.48, No.9, September 2001.

[33] I. Diagne, B Fleur, M. O Sidya, S. Gaye, G. SISSOKO (2008)
Détermination de Paramètres Thermiques d'un Matériau en Régime Dynamique Fréquentiel à Partir de Diagrammes de Bode et de Représentation de Nyquist
Journal des Sciences, Vol. 8, N°2 pp88-98

[34] K. OuldCheikh, I. Diagne, M. L. Sow, M. S. OuldBrahim, A. Diouf, K. Diallo, M. Dieng and G. Sissoko, 2013
Interpretation of the Phenomena of Heat Transfer from Representations of Nyquist and Bode Plots
Research Journal of Applied Sciences, Engineering and Technology 5(4): 1118-1122,